



# Statistical Properties of Fracture Precursors

A Garcimartín, Alessio Guarino, L Bellon, S Ciliberto

## ► To cite this version:

A Garcimartín, Alessio Guarino, L Bellon, S Ciliberto. Statistical Properties of Fracture Precursors. Biophysical Reviews and Letters, 1997, 79 (17), 10.1103/PhysRevLett.79.3202 . hal-01228881

**HAL Id: hal-01228881**

**<https://hal.univ-reunion.fr/hal-01228881>**

Submitted on 27 Feb 2016

**HAL** is a multi-disciplinary open access archive for the deposit and dissemination of scientific research documents, whether they are published or not. The documents may come from teaching and research institutions in France or abroad, or from public or private research centers.

L'archive ouverte pluridisciplinaire **HAL**, est destinée au dépôt et à la diffusion de documents scientifiques de niveau recherche, publiés ou non, émanant des établissements d'enseignement et de recherche français ou étrangers, des laboratoires publics ou privés.

## Statistical Properties of Fracture Precursors

A. Garcimartín,\* A. Guarino, L. Bellon, and S. Ciliberto†

*Laboratoire de Physique, Ecole Normale Supérieure de Lyon, 46, allée d'Italie, 69364 Lyon Cedex 07, France*

(Received 4 June 1997)

We present the data of a mode-I fracture experiment. The samples are broken under imposed pressure. The acoustic emission of microfractures before the breakup of the sample is registered. From the acoustic signals, the position of microfractures and the energy released are calculated. A measure of the clustering of microfractures yields information about the critical load. The statistics from energy measurements strongly suggest that the fracture can be viewed as a critical phenomenon; energy events are distributed in magnitude as a power law, and a critical exponent is found for the energy near fracture. [S0031-9007(97)04346-9]

PACS numbers: 62.20.Mk, 46.30.Nz

Fracture is a problem which has recently received a lot of attention in the physics community [1–3]. It is troublesome to calculate the force needed to break a heterogeneous material. Instead, it is customary to resort to tests involving the destruction of the sample. Therefore it is interesting to provide additional knowledge about cracks by studying the events that occur prior to the fracture. Besides, despite great experimental and numerical efforts [1–6], many aspects still remain unclear about the fracture process itself. Conceptually simple models, such as percolation [6] and self-organized criticality [7], are attractive but often fail to convey the complex phenomenology observed. The main motivation of this work is to understand if these models can reproduce the main features of crack formation.

We report here some experimental results that may help to gain valuable information in that direction. Our main tool is the monitoring of the microfractures, which occur before the final breakup, by recording their acoustic emissions (AE). Because of its ability to pinpoint the emission source, this technique has been widely used in seismography and to map the nucleation of fractures [8]. From these signals, we have also obtained the acoustic energy of each microfracture, which is a fraction of the total energy released. The behavior of the energy just before fracture is a good parameter to compare with the above mentioned models.

In order to avoid noise, we have designed a setup in which there are no moving parts, the force being exerted by pressurized air (see Fig. 1). A circular sample having a diameter of 22 cm and a thickness of 5 mm is placed between two chambers between which a pressure difference  $P = P_2 - P_1$  is imposed. The deformation of the plate at the center is bigger than its thickness, then the load is mainly radial [9,10]. Therefore, the experience can be thought of as a mode-I test with circular symmetry. The pressure difference  $P$  supported by the sample is slowly increased and it is monitored by a differential transducer. This measure has a stability of 0.002 atm. The fracture pressure for the different tested materials ranges from 0.7 to 2 atm. We regulate  $P$  by means of

a feedback loop and an electronically controlled valve which connects one of the two chambers to a pressurized air reservoir. The time taken to correct pressure variations (about 0.1 s) is smaller than the characteristic time of the strain rate. An inductive displacement sensor gives the deformation at the center of the plate with a precision of about 10  $\mu\text{m}$  (the deformation just before fracture is of the order of 1 cm). The apparatus is placed inside a copper box covered with a thick foam layer to avoid both electrical and acoustical noise. Four wide-band piezoelectric microphones are placed on the side of the sample (see Fig. 1). The signal is amplified, low-pass filtered at 70 kHz, and sent to a digitizing oscilloscope and to an electronic device which measures the acoustic energy detected by the microphones. The signal captured by the oscilloscope is sent to a computer where a program automatically detects the arrival time of the AE at each microphone. Afterwards, a calculation yields the position of the source inside the sample. A fraction of the detected events is rejected, either as a result of a large uncertainty of the location, or because they are regarded as noise. The mean standard error for the calculated positions is about 6 mm, which results mainly from the uncertainty of the arrival time. The electronic device that measures the energy performs the square of the AE amplitude and then integrates it over a time window of 30 ms, which is the maximum duration of one acoustic event. The output signal is proportional to the energy of the events [11], and

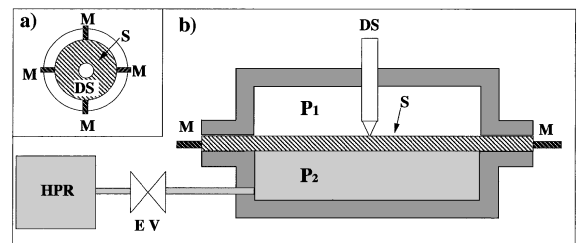


FIG. 1. Sketch of the setup. (a) Top view. S: sample; M: microphones; DS: displacement sensor. (b) Side view. EV: electronic valve. HPR: high pressure reservoir.

its value is sent to the computer. The dynamic range for the energy measurement is four decades, and the device is adjusted in such a way that only the strong sound emitted by the final crack saturates it. The global results of the measurements are the following: a list of the positions of microfractures, the strain of the samples, and the energy released as a function of  $P$ . Further details of the setup will be described elsewhere [12].

The loading can be applied in several ways. In order to allow comparison with some numerical models (specially those involving fuse networks, see, for example, [3,13]), we load the sample in such a way that  $P$  is imposed and slowly increased. The analogy with a fuse network goes like this: the electric current is formally equivalent to the stress, the voltage across the lattice to the strain, and the conductivity to the Young modulus. Our experiment corresponds to a situation where current is imposed and voltage is the dependent variable, which is the standard situation in numerical simulations. This is important because the features of energy near fracture are different if displacement, instead of pressure, is imposed, as is often done in fracture experiments. Energy from AE released by fractures has been studied in many different situations: in granite [8], in volcanoes [14], in chemically induced fracture [15], in plaster samples cracked by piercing through them [16], and in the explosion of a spherical tank [17]. In our experiment we pay special attention to the following points. First, we place ourselves in a clearly defined situation, namely, mode-I fracture. Second, we follow a load procedure in which we impose the control parameter. Third, we take care to ensure that the energy detected, which is the “order parameter,” is not contaminated from noise.

The samples are made of composite inhomogeneous materials, such as plaster, wood, or fiberglass. The experimental results are similar for all the materials. In this paper we present results for chipboard wood plates, which are most representative of the observed behavior. The chipboard we employed is made of glued short fibers randomly oriented, and cracks when stressed without defoliating. Each run is carried out in the following way. A sample is placed in the apparatus and a pressure ramp is applied. The rate of pressure increase, which is adjusted so that the succession of microfractures does not proceed too fast, is about 0.5 atm/h. In this way, the run lasts for about 2 h. In several runs, we have changed the pressure increase rate so that the sample cracks after a time spanning from 30 min to 5 h without noticing significant differences. However, if the sample is loaded, then unloaded before fracture, and loaded again, only a small number of microfractures are detected before attaining the previous load (Kaiser effect). In all the runs reported here, we have increased the pressure monotonically. Several hundreds, even thousands, of microfractures are detected prior to the destruction of the sample.

With the data acquired we are able to replay a “movie” of the run, plotting the location of the microfractures as the

pressure is increased (Fig. 2). Figures 2(a)–2(e) show the localization of microfractures at pressure intervals  $(m - 1)/5 < p < m/5$ , where  $m = 1, \dots, 5$  and  $p = P/P_c$  is the normalized pressure,  $P_c$  being the fracture pressure. Figure 2(f) shows all the microfractures registered. The final distribution of microfractures agrees well with the observed crack pattern. It has been noticed [8] that as the applied stress is increased, microfractures tend to nucleate and form a major fault, eventually causing the failure of the material. If microfractures are tightly clustered, it can be suspected that the material is severely damaged. It is therefore natural to try to quantify the extent to which microfractures are grouped together. Several measures of disorder have been proposed [18,19] that can be applied to this case. We have proceeded as follows. We look for the distribution of microfractures that happen within a given pressure interval. The sample surface is divided in squares and the number of microfractures  $n_i$  inside each square is evaluated. The entropy  $S$  is then computed:  $S = -\sum_i q_i \ln q_i$ , where  $q_i = n_i/N$ ,  $N$  being the total number of microfractures in the pressure interval. To compare between different pressure intervals, each of them having a different number of microfractures, the entropy for each interval is normalized to the equipartition entropy  $S_e$  (the entropy of  $N$  events evenly distributed through the grid), so a normalized entropy  $s = S/S_e$  is obtained. The values  $s = 1$  and  $s = 0$  correspond, respectively, to total disorder and extreme concentration. We have used a grid containing a number of squares of the same order as the average  $N$ . In this way, the smallest structure that can be detected has a size of about 2 cm, which is slightly larger than the typical size of the clusters of microfractures. The value of  $s$  slightly depends on the grid size; the aspect of the curve, however, remains the same for the different grids we have used.

In Fig. 3  $s$  is plotted versus  $p$ . It can be seen that  $s$  monotonically decreases as the control parameter is increased. In this way, the extent to which faults have

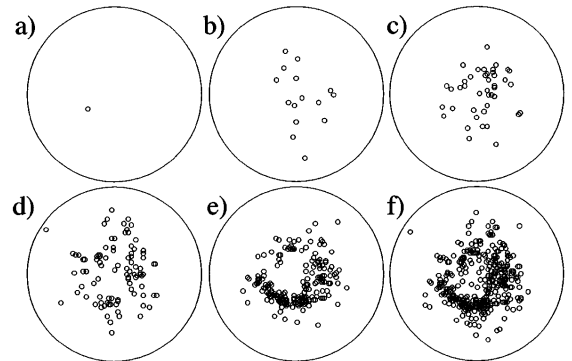


FIG. 2. Localization of microfractures for one sample as  $P$  is increased. The microfractures occurring at five equal pressure intervals are represented in (a)–(e). Pressure grows from (a) to (e). In (f) all the microfractures occurring during the run are plotted.

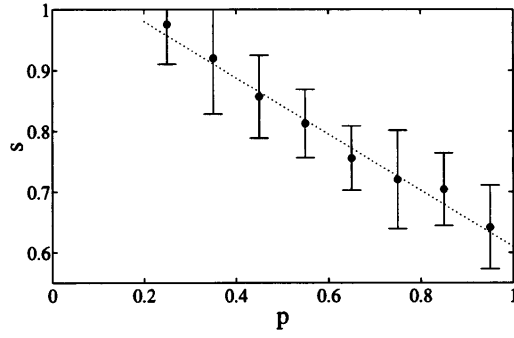


FIG. 3. Normalized entropy  $s$  versus  $p$ . The linear fit (dashed line) is a guide for the eye. Eleven samples were used to calculate the average and the error bars. (For pressures less than  $p = 0.2$ , it is not possible to calculate  $s$  due to the small number of microfractures.)

developed can be grasped. This measure may provide a nondestructive, albeit damaging test. While this is valid for the other materials we have tested, we are not in a position to state that the decrease of entropy follows in all cases the same law. More work is needed to develop this method, but with present results the point where half the critical pressure is reached can be already predicted with an error of  $\pm 20\%$  at  $s \approx 0.8$  (see Fig. 3).

We now study the behavior of the released energy as a function of  $P$ . The instantaneous energy  $\varepsilon$  released by a sample is shown in Fig. 4(a) as a function of  $p$ . The energy signal consists of bursts, which correspond to microcracks. In particular, we are interested in analyzing the dependence on  $P$  of the energy near fracture. In percolation models, the order parameter diverges following a power law as the control parameter is increased. A critical exponent is then found. This is valid only close to the phase transition, say within 5% of the critical value. To do this, we first calculate the cumulated energy  $E$ , i.e., the total energy released up to a pressure  $P$ . We then search a law in the form  $E = E_0 \left( \frac{P_c - P}{P_c} \right)^{-\alpha}$ , where  $E_0$  and  $\alpha$  are constants to be fitted. In Fig. 4(b) we present such a fit for the normalized data of 11 wood samples. We obtain  $\alpha = 0.27 \pm 0.05$ . This value shows small variations between different samples of the same material but presents a little dependency on the material. For fiberglass, for instance,  $\alpha = 0.22 \pm 0.05$ . This is not surprising since the behavior near the critical point, even in numerical models [6], is expected to depend strongly on microscopic features such as the geometry and the type of the bonds. It would be tempting to compare this figure to other exponents obtained in percolation models [6,13] or in other experiments [17]. This would not be reasonable, given the sensitivity to the specific details of the model. Nevertheless, the power law behavior is clearly seen close to  $P_c$ . This is a good indicator that fracture could be modeled using those frameworks, and described as a critical phenomenon.

The probability density function for  $\varepsilon$  is plotted in Fig. 4(c). The upper and lower energy limits are, respec-

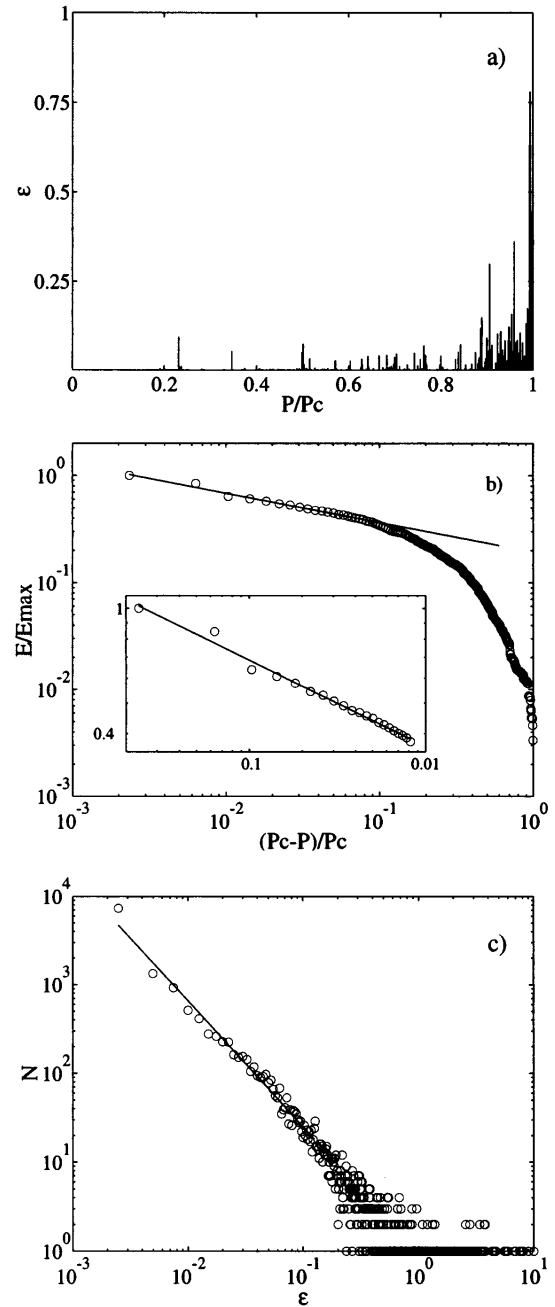


FIG. 4. (a) The energy released  $\varepsilon$  as a function of  $p$  for one of the samples. Energy bursts correspond to microfractures. (b) Cumulated normalized energy  $E/E_{\max}$  versus reduced pressure  $(P_c - P)/P_c$ , where  $E_{\max}$  is the total energy. A power fit has been done near  $P_c$  (solid line). The inset is a zoom near  $P_c$ . (c) Histogram of  $\varepsilon$  from the events registered in 11 wood plates. Energy intervals have a width of 5 times the measurement precision. The fit  $\ln N = \ln \varepsilon_0 - \gamma \ln \varepsilon$  is shown.

tively, the strongest event recorded and the noise level. A power law is obtained spanning through more than two decades. This has also been observed in numerical

simulations of the fracture of a bundle of fibers [20]. Again the exponent shows little variation between different samples of the same material. For wood, the exponent is  $\gamma = -1.51 \pm 0.05$ . This value compares well to the one given in [7] and [21], but it differs a little from one material to another. For fiberglass, for example,  $\gamma = -2.0 \pm 0.1$ . Even if the exponent agreement is coincidental or if it is not universal, the power law behavior strongly suggests a critical dynamics. An important remark should be made here. This feature may depend on the experimental procedure. In our experiment  $P$  is imposed and slowly increased, and this may easily trigger an avalanche, as in the scenario of self-organized criticality. If the loading is instead carried out by slowly increasing the strain, the power law might not be found. A detailed discussion about the dependence of the results on the loading methods will be treated in a forthcoming article [12].

In summary, we have presented experimental data showing a strong analogy between the formation of a crack in composite materials and percolation in a fuse network. On a qualitative level the microcracks clusterize around the final crack. On a more quantitative level, if the system is driven at imposed pressure, the data show the existence of a critical exponent for the energy released by microfractures near the critical point, supporting the view that fracture can be thought of as a critical phenomenon. We have also shown that the probability density function of the energy can be fitted by a power law. Finally, we propose that the localization entropy can provide some information about the critical load before the fracture is reached.

This work has been partially funded by Contracts No. ERBCHRX940546 and No. ERBFMBICT950126 from the European Community. We acknowledge useful discussions with R. Livi, A. Politi, and S. Roux, and technical support by J.L. DeMarinis, M. Moulin, and F. Vittoz.

---

\*Permanent address: Departamento de Física, Facultad de Ciencias, Universidad de Navarra, E-31080 Pamplona, Spain.

†Author to whom all correspondence should be addressed. Electronic address: cilibe@physique.ens-lyon.fr

- [1] J. Fineberg, S.P. Gross, M. Marder, and H.L. Swinney, Phys. Rev. B **45**, 5146 (1992); J.F. Boudet, S. Ciliberto, and V. Steinberg, Europhys. Lett. **30**, 337 (1995); M. Marder, Nature (London) **381**, 275 (1996).

- [2] A. Ometchenko, J. Yu, R.K. Kalia, and P. Vashista, Phys. Rev. Lett. **78**, 2148 (1997); F.F. Abraham, Europhys. Lett. **38**, 103 (1997).
- [3] S. Zapperi, P. Ray, H.E. Stanley, and A. Vespignani, Phys. Rev. Lett. **78**, 1408 (1997).
- [4] M.F. Kanninen and C.H. Popelar, *Advanced Fracture Mechanics* (Oxford University Press, New York, 1985).
- [5] B. Lawn, *Fracture of Brittle Solids* (Cambridge University Press, Cambridge, 1993), 2nd ed.
- [6] *Statistical Models for the Fracture of Disordered Media*, edited by H.J. Herrmann and S. Roux (North-Holland, Amsterdam, 1990).
- [7] P. Bak, C. Tang, and K. Wiesenfeld, Phys. Rev. Lett. **59**, 381 (1987); Phys. Rev. A **38**, 364 (1988).
- [8] D.A. Lockner, J.D. Byerlee, V. Kuksenko, A. Ponomarev, and A. Sidorin, Nature (London) **350**, 39 (1991).
- [9] L.D. Landau and E.M. Lifshitz, *Theory of Elasticity*, Course of Theoretical Physics Vol. 7 (Pergamon, London, 1959).
- [10] S.P. Timoshenko and S. Woinowsky-Krieger, *Theory of Plates and Shells*, Engineering Mechanics Series (McGraw-Hill, New York, 1959), 2nd ed.
- [11] This is strictly true only if there is no attenuation. We have measured the attenuation coefficient, and we found that it is very small. For wood, a correction of at most 5% would be needed. We have not taken this effect into account. Moreover, no directionality has been observed in the acoustic emission.
- [12] A. Guarino, A. Garcimartín, and S. Ciliberto (to be published).
- [13] D. Sornette and C. Vanneste, Phys. Rev. Lett. **68**, 612 (1992).
- [14] P. Diodati, F. Marchesoni, and S. Piazza, Phys. Rev. Lett. **67**, 2239 (1991).
- [15] G. Cannelli, R. Cantelli, and F. Cordero, Phys. Rev. Lett. **70**, 3923 (1993).
- [16] A. Petri, G. Paparo, A. Vespignani, A. Alippi, and M. Constantini, Phys. Rev. Lett. **73**, 3423 (1994).
- [17] J.-C. Anifrani, C. Le Floch, D. Sornette, and B. Souillard, J. Phys. I (France) **5**, 631 (1995).
- [18] R. López-Ruiz, H.L. Mancini, and X. Calvet, Phys. Lett. A **209**, 321 (1995).
- [19] A.O. Hero and O. Michel, in Proceedings of the International Symposium on Information Theory, Ulm, Germany, 1997 (to be published).
- [20] P.C. Hemmer and A. Hansen, J. Appl. Mech. **59**, 909 (1992); M. Kloster, A. Hansen, and P.C. Hemmer, "Burst Avalanches in Solvable Models of Fibrous Materials."
- [21] G. Caldarelli, F.D. Di Tolla, and A. Petri, Phys. Rev. Lett. **77**, 2503 (1996).